## Supplementary Material

1. Data acquisition
2. Figures S1 to S4
3. Table S1 to S2

## Introduction

The supporting information presented here includes an extended method on the data acquisition and abstraction time-series.

## Data acquisition

### Precipitation and potential evapotranspiration

We obtained monthly mean precipitation and PET series for all 43 districts in the study area within the states of Punjab and Haryana from the Indian Meteorological Department for the period 1951-2010. Monthly mean precipitation data for less than 4% spread over all districts were missing for the period 2006-2010; for those missing districts and months we used linear interpolation of values from neighboring districts. $PET$ between 1951 and 2010 was calculated using mean temperature ($T_{mean}$), net radiation ($R_{net}$), and ground heat flux ($G$) according to Allen et al. (1998). Monthly mean precipitation and $PET$ were then converted into daily values (in units of mm/day) as model input by uniformly distributing them over each month. District-wide values were interpolated onto a uniform 10 x 10 km grid over the study area (Figures S3a and b) by determining the dominant district associated with each grid cell. The spatial distribution of mean precipitation is related to topographic elevation, with higher rates in the northeast where the land surface rises towards the Himalayan front. Similarly, PET is topographically controlled; rates reduce to the northeast as the land surface rises towards the Himalaya and mean temperatures decrease.
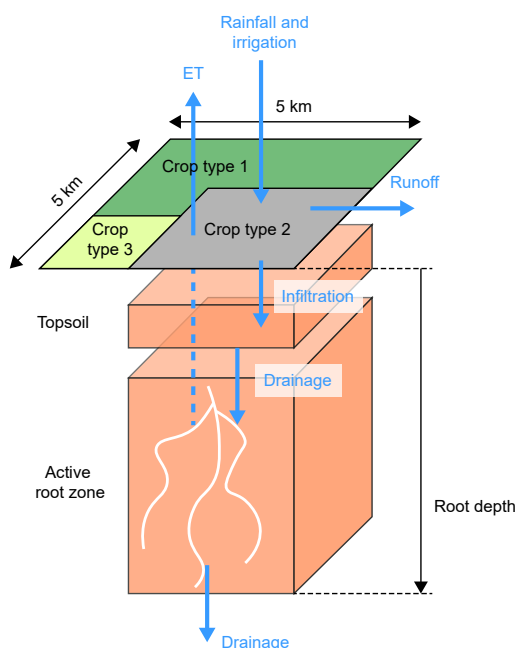
**Table S1.** Calibrated irrigation efficiencies (CIE) for each crop type

| Crop type from Moulds et al. (2018) | CIE (-) |
|---|---|
| Bajra | 0.7 |
| Barley | 0.7 |
| Cotton | 0.3 |
| Fruit | 0.35 |
| Gram | 0.62 |
| Groundnut | 0.7 |
| Maize | 0.7 |
| Other cereal (kharif) | 0.7 |
| Ohter cereal (rabi) | 0.3 |
| Other pulse (kharif) | 0.3 |
| Other pulse (rabi) | 0.41 |
| Ragi | 0.3 |
| Rapeseed | 0.5 |
| Rice (autumn) | 0.69 |
| Rice (summer) | 0.7 |
| Rice (winter) | 0.7 |
| Sorghum (kharif) | 0.35 |
| Sorghum (rabi) | 0.36 |
| Sugarcane | 0.7 |

### Abstraction

Estimation of total groundwater abstraction (billion cubic meters, bcm) has been carried out by the Central Groundwater Board (CGWB) using tube well density records for all districts in the study area for the years 2004, 2009, and 2011 (CGWB 2006, 2011, 2014). To simulate the groundwater level dynamics, however, we require monthly mean abstraction data across the region, which have not been previously reported. An alternative approach to estimating monthly groundwater abstraction for irrigation is to calculate the deficit between crop water requirements and effective precipitation, as demonstrated for example by Daccache and others Daccache et al. (2014). We adopted this approach, using the soil water balance model of Hess et al. (2000) and India-wide annual land use/land cover maps produced by Moulds (2016) for the period 1951 to 2010 with the toolbox of Moulds et al. (2015). For more detail see below. This provided us with a time series of monthly mean groundwater abstraction volumes per 5 x 5 km grid cells (bcm) over the period 1950-2010, which was recalculated for our 10 x 10 km grid (Figure S3c). We assumed that abstraction rates prior to this period are the same as those for 1951. Modeled abstraction rates are highest in the northern part of the study area with a general decline towards the south and away from the Himalayan front. Our map of modeled mean abstraction shows the same spatial pattern as that derived by Cheema et al. (2014), who used the Soil Water Assessment Tool (SWAT) model to estimate groundwater abstraction for 2007 for the states of Punjab and Haryana.

Daily gridded groundwater abstraction time-series were produced using the WaSim one-dimensional soil water balance and crop water demand model (Hess et al. 2000), which has been used in the past to simulate irrigation requirements (Knox et al. 1997), groundwater recharge (Holman et al. 2009) and for catchment land use and water balance studies in temperate (Hess et al. 2010; Holman et al. 2011) and semi-arid (Gada 2014) environments. The original WaSim code includes four subsurface layers consisting of a topsoil layer, an active root zone, unsaturated zone and a
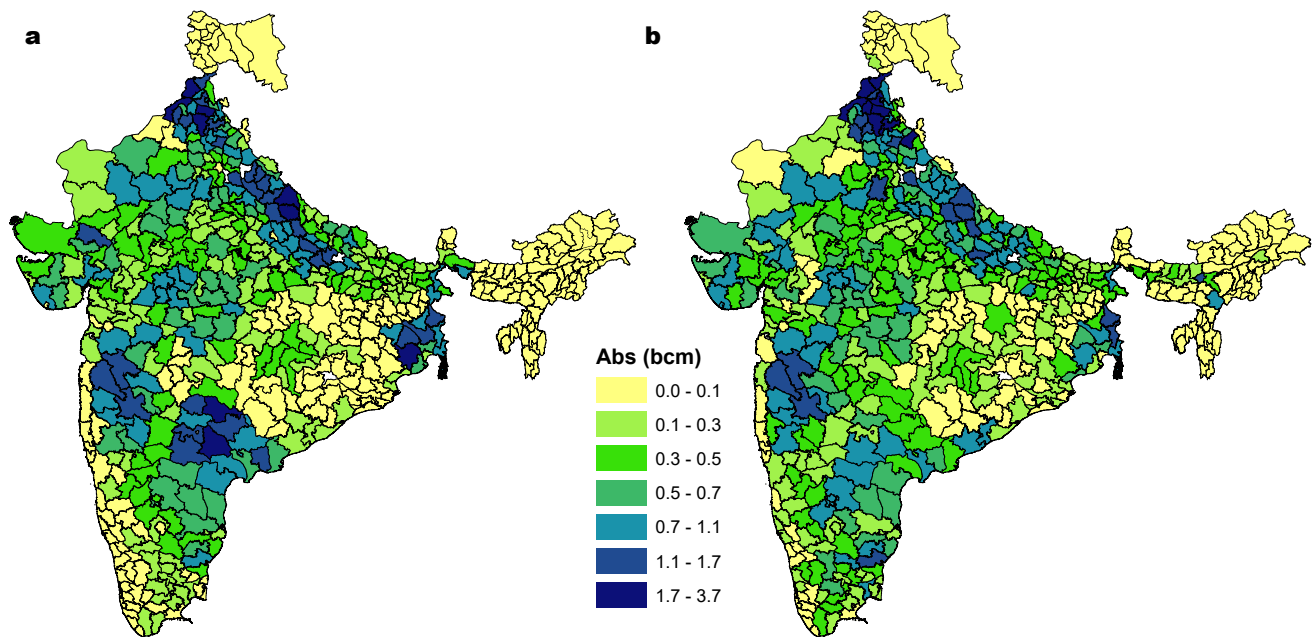


**Figure S1.** Structure of a single model grid cell of the simplified WaSim model.

**Figure S2.** Simulated (a) and observed (b) district-wise annual groundwater abstraction for the year 2011 in billions of cubic meters (bcm).

saturated zone layer. In this study, a simplified version of the model was implemented which only includes the topsoil and active root zone layers. A description of the model structure and the datasets used to parameterise and drive the model is provided below. Hess et al. (2000) provide a full description of the model and the equations that underpin it.

The simplified WaSim model was implemented on a 5 km grid across the whole of India. Each grid cell includes parameterisations of the land surface (crop types), topsoil and active root zone (Figure S1). Within each grid cell the soil type is fixed, but the land surface may consist of multiple crop types that can change over time. The soil water balance is solved for each of these crop types separately.

The model was driven by daily gridded rainfall and potential evapotranspiration data from 1951 to 2014. Rainfall time-series for each cell were derived by combining two datasets. For the period 1951 – 1997 data were extracted from the Indian Meteorological Department's 1° daily gridded dataset (Rajeevan et al. 2006). For the period 1998 – 2014 daily rainfall values were derived from Tropical Rainfall Measuring Mission (TRMM) 3B42-V7 dataset (Huffman et al. 2007). Daily potential evapotranspiration (PET) rates were also constructed from two data sets. Between 2000 and 2014 values were obtained from NASA's MOD16A2 Version 6 Evapotranspiration/Latent Heat Flux product (ORNL DAAC 2018). Between 1951 and 1999 values were extracted from the CRU TS3.21 dataset (Harris et al. 2014), which were then bias-corrected against the MODIS data using the equidistant quantile matching approach of Li et al. (2010).

The soil receives water from infiltration of rainfall and irrigation water. Infiltration is calculated as the gross input minus surface runoff. Any water that falls onto saturated soil is assumed to runoff due to saturation excess. Infiltration excess runoff is also simulated using the SCS-curve method (Hawkins et al. 1985).

The soil loses water by three main mechanisms. Firstly, water can evaporate directly from the topsoil based on the method of Ritchie (1972). Transpiration from the active root zone also contributes to losses, the rate of which depends on soil water availability and crop water demand. Finally, if the active root zone water content exceeds field capacity, a portion of the excess will drain based on the exponential relationship developed by Raes and van Aelst (1985).

Annual gridded crop coverage maps produced by Moulds et al. (2018) were used to update the land surface parameterisation of the model each year. These maps include the proportional coverage of 23 different crop types across India. To account for the dynamic intra-annual development of crop coverage and water demand, quantitative information on crop growth cycles, water requirements (Brouwer and Heibloem 1985) and root depth (Allen et al. 1998) were used to parameterise these aspects of the model. Soil storage capacity and drainage behaviour was parameterised using hydraulic properties of soil texture classes (Saxton and Rawls 2006) in conjunction with the global map of soil texture produced as part of the Harmonized World Soil Database (Fischer et al. 2008).

The scheduling of irrigation was based on the detailed field survey of Indian irrigation strategies undertaken by O'Keeffe et al. (2016). They found that rather than satisfying crop water requirements on a daily basis, farmers tend to saturate (or even pond) the soil and then wait for a number of days before they irrigate again. Furthermore, the time between irrigation depends on the water demand of the crop and climatic conditions. Accordingly, it was decided to include a scheduling system in the model that assumes that farmers apply irrigation up to the field capacity of the soil. Once this is reached, they will wait until the plants become stressed under dry soil conditions (permanent wilting point) before irrigating again. For rice paddy fields there is the additional preparation required whereby, the field is flooded. This was
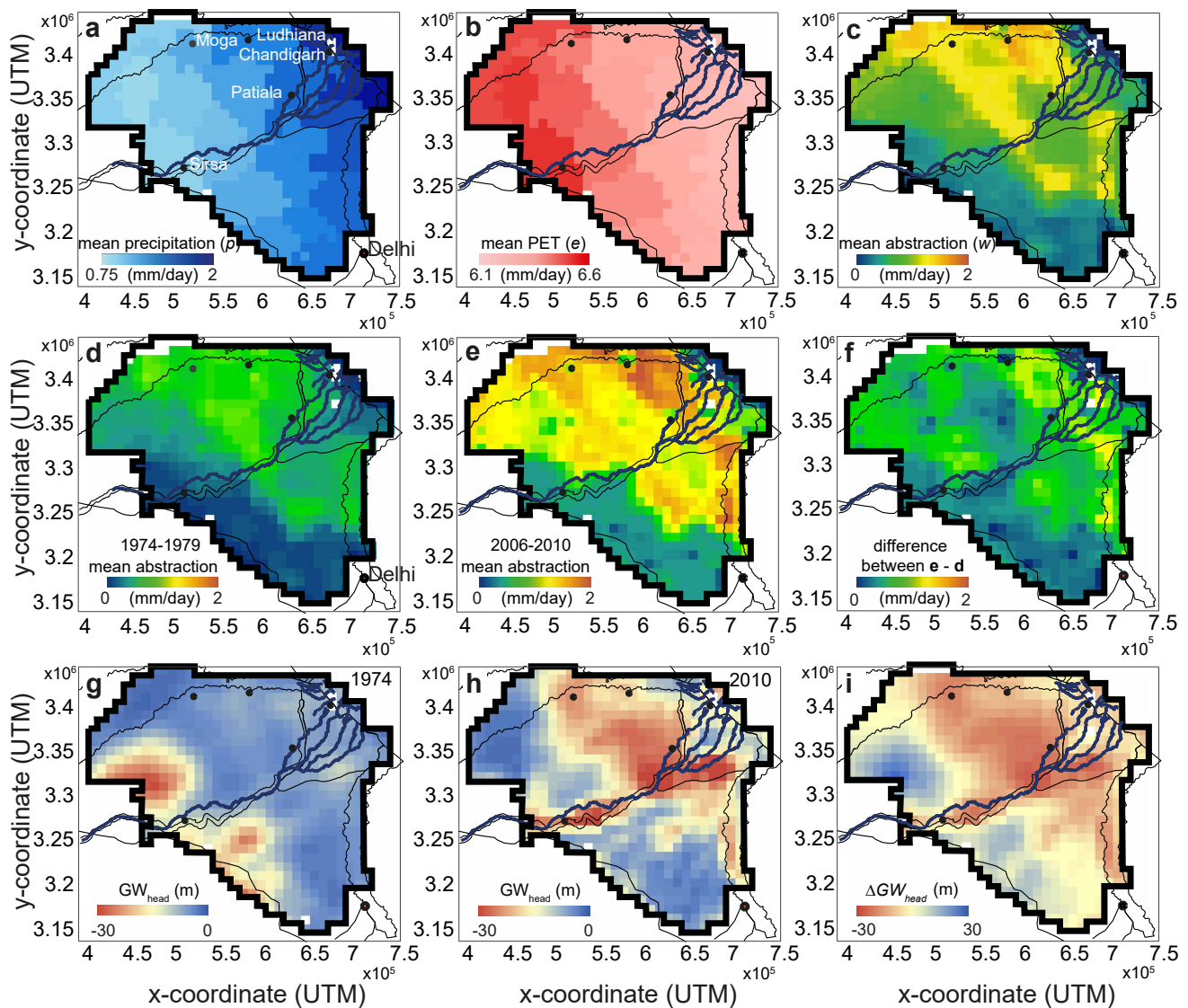
**Figure S3.** Maps of 10 x 10 km gridded mean (a) precipitation ($p$) and (b) PET ($e$) for 1974-2010, mean abstraction ($w$) for (c) 1974-2010, (d) 1974-1979, (e) 2006-2010, (f) the difference in abstraction between these two five-year periods, the mean groundwater level for (g) 1974 and (h) 2010, and (i) the change in groundwater level between 1974 and 2010.

accounted for by assuming that farmers maintain a 20 cm pond of water on the fields.

The model was run on a daily time-step from 1951 to 2014 and a daily gridded time-series of total irrigation was produced. Moulds et al. (2018) also produced gridded time-series of the proportion of irrigation water taken from groundwater. These data were used to convert the estimated total irrigation time-series into groundwater abstraction. A key source of uncertainty in the estimated groundwater abstracted is the irrigation efficiency i.e. the proportion of the total irrigation applied that is beneficially used by the crop. Inefficiencies may stem from the leakages in the conveyance system or other equipment and other external factors not included in the model such as wind drift losses. Field studies indicate that they often depend on the particular type of irrigation method employed (Martin and Gilley 1993) and can range from 30 to 90% (Narayanamoorthy 2009). Accordingly, this parameter was calibrated on a crop by crop basis using the Indian Central Ground Water Board estimates of district-wise groundwater abstraction for the year 2011

as a calibration dataset (Table S1). Figure S2 compares the simulated and observed 2011 groundwater abstraction for each district of India. The model captures the spatial distribution of groundwater abstraction and achieves a R2 score of 0.58 indicating that it captures just under 60% of the variance in district-wise abstraction data. Overall, the model shows a small negative bias of 0.03 billion cubic meters (bcm).

### Groundwater level data

The data were collected for the period 1974-2010 from borehole databases maintained by the state groundwater departments of Haryana and Punjab, and by the CGWB. The state water level data contain measurements from boreholes taken twice a year in June and October since 1973. The CGWB data contain levels measured in boreholes approximately four times each year, typically in January, May, August and November, from 2002 to 2010. Joshi et al. (In review) compiled observations from 4417 wells for the period of 1974-2010 and prepared pre-monsoon (May-June)
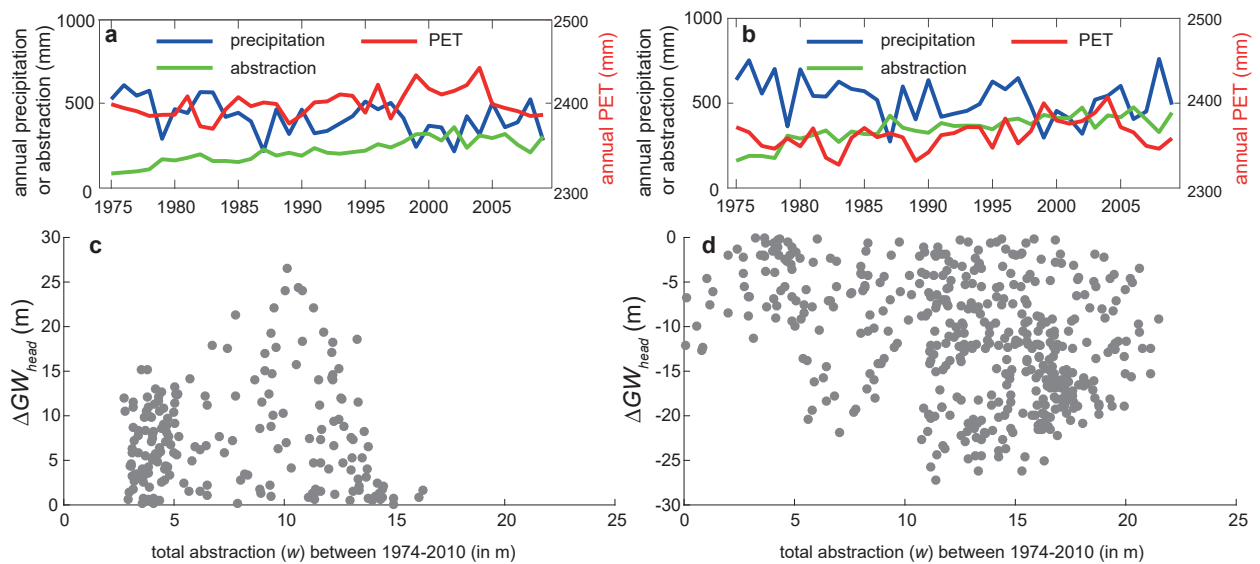
**Figure S4.** Relationships between precipitation, PET, abstraction, and groundwater level changes. a) Annual precipitation, abstraction and PET for grid cells in group 1 that show groundwater level rise over the period 1974-2010. (b) Annual precipitation, abstraction and PET for grid cells in group 2 that show groundwater level fall. (c) Groundwater level change plotted against total abstraction over the period 1974-2010 for grid cells in group 1. Note the lack of a clear relationship. (d) Groundwater level change plotted against total abstraction for grid cells in group 2. Note the general decline in water level with increasing total abstraction, albeit with high levels of scatter.

and post-monsoon (October-November) groundwater level maps at a grid cell resolution of 1.5 km using a kriging geostatistical approach. For the modeling described here, we averaged the groundwater levels maps to our 10 x 10 km grid. Pre-monsoon water levels for 1974 and 2010 are shown in Figures S3g and S3h.

Groundwater levels in 1974 were generally within  2 m of the surface across much of the study area, except in the south west where they could be up to  30 m below ground (Figure S3g). The groundwater level surface for 2010 (Figure S3h) is notably different, with deep (20-30 m) groundwater levels in much of the northern part of the study area and along the Ghaggar–Hakra paleochannel (Figure 1, Singh et al. 2017). The difference between these two surfaces (Figure S3i) shows the change in the groundwater table, which can be separated into two distinct zones ; water levels in the northeast have generally declined, while those in the southwest lvels have generally risen. This pattern broadly matches the spatial variation in mean abstraction rates, with higher abstraction rates in the north and east where groundwater levels have declined (Figure S3).

To begin to explore the relationships between precipitation, PET, abstraction, and water level change, we extract values of these variables for two groups of grid cells: those

– where groundwater levels have risen over the period 1974-2010 (group 1) and those where levels have declined (group 2). This initial analysis ignores the spatial variations in and correlations between variables, and considers only their variation in time. Time series of annual mean precipitation, PET and abstraction are plotted for these two groups in Figure S4. Visual inspection of these series suggests declining trends in the precipitation and rising trends in abstraction for both groups. We use the Mann-Kendall test (Hipel and McLeod 1994) to estimate Kendall's $\tau$ and its significance level for each time series trend within each group of cells (Table S2). This identifies trends in PET and abstraction that are significant at the $p=0.05$ level in the PET and abstraction timeseries for both groups. Precipitation trends are significant at $p=0.11$ for group 1 and $p=0.08$ for group 2. We use the Sen slope (Sen 1968) to estimate the change in these driving variables between 1974 and 2010. For PET this is negligible (+0.6 and +0.7 mm/year for group 1 and 2, respectively); for abstraction, the change is +6.5 and +6.1 mm/year for group 1 and 2, respectively; and for precipitation it is -4.7 and -3.7 mm/year for group 1 and 2, respectively. Averaging the abstraction rates over the start period (1974-1979) and end period (2006-2010) for the two groups of cells shows that has abstraction rates have risen from 104 to 272 mm/year across group 1 cells, and from 205 to 414 mm/year across group 2.

There appears to be little correlation between total groundwater abstraction over the period 1974-2010 and rise in groundwater level for cells in group 1 (Figure S4c), with a correlation coefficient of 0.03. In contrast, there is a weak negative relationship between total abstraction and decline in groundwater level for cells in group 2, with a correlation coefficient of -0.34 (Figure S4d). Trend lines of this relationship for group 2 cells, as estimated by Sen's method and by linear regression with the intercept

**Table S2.** Results of Mann-Kendall trend test and Sen's slope

| Variable | Mean (mm/yr) | $\tau$ | $p$ | Sen's slope (mm/yr) |
|---|---|---|---|---|
| Rainfall (group 1) | 416 | -0.31 | 0.11 | -4.7 |
| Rainfall (group 2) | 526 | -0.21 | 0.08 | -3.7 |
| PET (group 1) | 2399 | 0.24 | 0.05 | 0.7 |
| PET (group 2) | 2362 | 0.25 | 0.04 | 0.6 |
| Abstraction (group 1) | 212 | 0.72 | 0.00 | 6.5 |
| Abstraction (group 2) | 350 | 0.67 | 0.00 | 6.1 |

set to zero, are -0.63 and -0.84, respectively, and the coefficient of determination ($r^2$) for the linear regression model is 0.12. To explore whether variations in total rainfall or PET could explain the groundwater decline in the group 2 cells over the observational period, two additional multiple linear regression models were constructed: the first using total abstraction and total rainfall as the independent variables, and the second using total abstraction, rainfall, and PET. These regressions were performed using the non-negative least squares (nnls) package in the R programming environment Mullen and Stokkum (2012) but did not identify models with higher $r^2$ values.

## References

Allen RG, Pereira LS, Raes D and Smith M (1998) Crop evapotranspiration: Guidelines for computing crop water requirements: FAO Irrigation and drainage paper 56. Technical report, Food and Agriculture Organization of the United Nations, Rome, Italy.

Brouwer C and Heibloem M (1985) Irrigation water management: Training manual No. 3: Irrigation water needs. Technical report, Food and Agriculture Organization of the United Nations, Rome, Italy.

CGWB (2006) Dynamic ground water resources of India (as on march, 2004). Technical report, Central Ground Water Board, Ministry of Water Resources, Government of India, Faridabad.

CGWB (2011) Dynamic ground water resources of India (as on 31 march, 2009). Technical report, Central Ground Water Board, Ministry of Water Resources, Government of India, Faridabad.

CGWB (2014) Dynamic ground water resources of India (as on 31 march, 2011). Technical report, Central Ground Water Board, Ministry of Water Resources, River Development & Ganga Rejuvenation, Government of India, Faridabad.

Cheema MJM, Immerzeel WW and Bastiaanssen WGM (2014) Spatial quantification of groundwater abstraction i the irrigated Indus basin. *Ground Water* 52(1): 25–36. DOI: 10.1111/gwat.12027.

Daccache A, Ciurana JS, Rodriguez Diaz JA and Knox JW (2014) Water and energy footprint of irrigated agriculture in the Mediterranean region. *Environmental Research Letters* 9(12): 124014. DOI:10.1088/1748-9326/9/12/124014.

Fischer G, Nachtergaele FO, Prieler S, Teixeira E, Tóth G, Van Velthuizen H, Verelst L and Wiberg D (2008) Global Agro-ecological Zones Assessment for Agriculture. Technical report, Food and Agriculture Organization of the United Nations, Rome, Italy.

Gada MA (2014) *Understanding the Water Balance of Basement Complex Areas in Sokoto Basin, North-West Nigeria for improved Groundwater Management*. PhD Thesis, Cranfield University.

Harris I, Jones PD, Osborn TJ and Lister DH (2014) Updated high-resolution grids of monthly climatic observations – the CRU TS3.10 Dataset. *International Journal of Climatology* 34(3): 623–642. DOI:10.1002/joc.3711.

Hawkins RH, Hjelmfelt Jr AT and Zevenbergen AW (1985) Runoff Probability, Storm Depth, and Curve Numbers. *Journal of Irrigation and Drainage Engineering* 111(4): 330–340. DOI: 10.1061/(ASCE)0733-9437(1985)111:4(330).

Hess T, Leeds-Harrison P and Counsell C (2000) *WaSim Technical Manual*. Wallingford, UK.

Hess TM, Holman IP, Rose SC, Rosolova Z and Parrott A (2010) Estimating the impact of rural land management changes on catchment runoff generation in England and Wales. *Hydrological Processes* 24(10): 1357–1368. DOI: 10.1002/hyp.7598.

Hipel KW and McLeod AI (1994) *Time series modelling of water resources and environmental systems*. Elsevier Science.

Holman IP, Hess TM and Rose SC (2011) A broad-scale assessment of the effect of improved soil management on catchment baseflow index. *Hydrological Processes* 25(16): 2563–2572. DOI:10.1002/hyp.8131.

Holman IP, Tascone D and Hess TM (2009) A comparison of stochastic and deterministic downscaling methods for modelling potential groundwater recharge under climate change in East Anglia, UK: implications for groundwater resource management. *Hydrogeology Journal* 17(7): 1629–1641. DOI:10.1007/s10040-009-0457-8.

Huffman GJ, Bolvin DT, Nelkin EJ and Wolff DB (2007) The TRMM Multisatellite Precipitation Analysis (TMPA): Quasi-Global, Multiyear, Combined-Sensor Precipitation Estimates at Fine Scales. *J. Hydrometeor.* 8: 38–55. DOI: 10.1175/JHM560.1.

Joshi SK, Rai S, Sinha R, Gupta S, Shekhar S, Rawat YS, Kumar M, Mason PJ, Densmore AL, Singh A, Nayak N and Van Dijk WM (In review) Spatio-temporal Variations in Groundwater Levels in Northwest India and Implications for Future Groundwater Management. *Water Resources Research* .

Knox JW, Weatherhead EK and Bradley RI (1997) Mapping the total volumetric irrigation water requirements in England and Wales. *Agricultural Water Management* 33(1): 1–18. DOI: 10.1016/S0378-3774(96)01285-1.

Li H, Sheffield J and Wood EF (2010) Bias correction of monthly precipitation and temperature fields from Intergovernmental Panel on Climate Change AR4 models using equidistant quantile matching. *Journal of Geophysical Research – Atmospheres* 115: D10101. DOI:10.1029/2009JD012882.

Martin L and Gilley JR (1993) Part 623 National Engineering Hand-book: Chapter 2 Irrigation Water Requirements. Technical report, United States Department for Agriculture, Washington, USA.

Moulds S (2016) *Toward integrated modelling systems to assess vulnerability of water resources under environmental change*. PhD Thesis, Imperical College London.

Moulds S, Buytaert W and Mijic A (2015) An open and extensible framework for spatially explicit land use change modelling: the lulcc R package. *Geoscientific Model Development* 8: 3215–3229. DOI:10.5194/gmd-8-3215-2015.

Moulds S, Buytaert W and Mijic A (2018) A spatio-temporal land use and land cover reconstruction for India from 1960–2010. *Nature: Scientific Data* 5: 180159. DOI: 10.1038/sdata.2018.159.

Mullen KM and Stokkum IHM (2012) *The Lawson-Hanson algorithm for non-negative least squares (NNLS)*, R package version 1.4 edition.

Narayanamoorthy A (2009) Water saving technologies as a demand management option: potentials, problems and prospects. In: Saleth RM (ed.) *Promoting Irrigation Demand Management in India: Potentials, Problems and Prospects*. Colombo: IWMI,

pp. 93–126.

O'Keeffe J, Buytaert W, Mijic A, Brozović and Sinha R (2016) The use of semi-structured interviews for the characterisation of farmer irrigation practices. *Hydrology and Earth System Science* 20: 1911–1924. DOI:10.5194/hess-20-1911-2016.

ORNL DAAC (2018) MODIS and VIIRS Land Products Global Subsetting and Visualization Tool. Technical report, ORNL DAAC, Oak Ridge, Tennessee, USA. DOI: 10.3334/ORNLDAAC/1379.

Rajeevan M, Bhate J, Kale JD and Lal B (2006) High resolution daily gridded rainfall data for the Indian region: Analysis of break and active monsoon spells. *Current Science* 91(3): 296–306.

Ritchie JT (1972) Model for predicting evaporation from a row crop with incomplete cover. *Water Resources Research* 8(5): 1204–1213. DOI:10.1029/WR008i005p01204.

Saxton KE and Rawls WJ (2006) Soil Water Characteristic Estimates by Texture and Organic Matter for Hydrologic Solutions. *Soil Science Society of America* 70: 1569–1578. DOI:10.2136/sssaj2005.0117.

Sen PK (1968) Estimates of the regression coefficient based on Kendall's Tau. *Journal of the American Statistical Association* 63(24): 1379–1389. DOI:10.2307/2285891.

Singh A, Thomson KJ, Sinha R, Buylaert JP, Carter A, Mark DF, Mason PJ, Densmore AL, Murray AS, Jain M, Paul D and Gupta S (2017) Counter-intuitive influence of Himalayan river morphodynamics on Indus Civilisation urban settlements. *Nature Communications* 8: 1617. DOI:10.1038/s41467-017-01643-9.